Optimal Design of Voltage-Frequency Controllers for Microgrids

Mostafa Farrokhabadi
BluWave-ai
Ottawa, Canada
m5farrok@uwaterloo.ca

John W. Simpson-Porco
University of Toronto
Toronto, Canada
jwsimpson@ece.utoronto.ca

Claudio A. Cañizares
University of Waterloo
Waterloo, Canada
ccanizares@uwaterloo.ca

***Abstract*—This paper presents a systematic control synthesis framework for an optimal voltage-based frequency control (VFC) in islanded/isolated microgrids. The problem of voltage-based frequency control is formulated as an optimal $\mathcal{H}_\infty$ controller synthesis for the linearized microgrid model. The validity of model-reduction steps in which the feeders are neglected is discussed, and various centralized/decentralized control architectures are investigated. Multiple simulation studies are performed in MATLAB/Simulink to test and compare the performances of the control architectures in a microgrid test system. Simulation results confirm the robustness of the VFC controller with respect to simplifications in the system model, and proposed system disturbances compared to a non-optimal VFC.**

***Index Terms*—Microgrids, frequency control, stability, robust control**

I. Introduction

A Microgrid is a cluster of loads and Distributed Energy Resources (DERs), including Renewable Energy Resources (RES) and Energy Storage Systems (ESS), that acts as a single controllable entity [1], [2]. Microgrids may operate in both grid-connected and islanded forms [3], and should be capable of seamless transition to islanded mode [4]. Isolated microgrids, such as those in remote communities, have no Point of Common Coupling (PCC) with a larger grid.

Frequency control is a major challenge in isolated/islanded microgrids, in particular those with a higher penetration of electronically-interfaced DERs. First, in such microgrids, mechanical rotational inertia is much lower compared to conventional networks, especially for high penetration of converter-based DERs, making them prone to large frequency deviations [5]. In addition, demand-supply balance is critical in microgrids, especially in isolated ones, due to the intermittent nature of RES [6], and the low number of generation units, which increases the risk of large disturbances due to generator outages [5]. Hence, an islanded/isolated microgrid experiences more frequent frequency deviations and a larger rate of change of frequency compared to a bulk power system. In this case, conventional frequency control techniques and tools, designed for large interconnected networks, may not be effective for microgrid frequency regulation, even in the presence of sufficient generation reserve [7].

In view of the aforementioned frequency control challenges, numerous original and/or supplementary control techniques have been proposed in the literature [8], [9], including droop-based methods [10], [11], distributed cooperative controls [12], and central and/or hierarchical communication-based controls [13], [14]. All these control techniques are focused on proper power sharing among multiple DERs. Recently, the concept of a dynamic Voltage-based Frequency Controller (VFC) was introduced in [15] and [16], where it is shown that VFC acts as a virtual flywheel in microgrids, and compensates for the active power mismatch by changing the system operating voltages, due to the voltage sensitivity of loads in microgrids. Thus, the VFC operates in parallel to other power sharing techniques, and provides supplementary frequency control. VFC is based on the strong coupling between voltage and frequency in microgrids, since due to the relatively short feeders of microgrids, voltage changes at the DERs terminals are quickly reflected on the load side, with limited voltage drops through the feeders, which in turn changes the system demand depending on the load voltage sensitivity indices [17], [18]. Thus, this tight voltage-frequency coupling is used to control frequency in the system by changing set-points of the voltage regulators (e.g., synchronous machine exciters).

This paper presents a systematic disturbance rejecting control synthesis for voltage-based frequency control in islanded/isolated microgrids. The concept introduced in [15] is formalized and extended to evaluate various architectures for VFC, investigating the impact of each architecture on system small- and large-perturbation stability. The current paper presents two major technical contributions. First, in Section II-B, a detailed discussion on the impact of feeders in microgrid studies is given, in particular for VFC synthesis. It has been previously argued that network in microgrids may not play a significant role in the performance of control and optimization techniques [19], in particular because feeders are short and their static capacity is much greater than the maximum system demand [20], [21]. Conditions under which network simplifications and/or elimination would be reasonable are identified and discussed.

The paper is organized as follows: Section II discusses a systematic framework for VFC design through LMI-based minimization of the $\mathcal{H}_\infty$ gain from active power disturbances to frequency deviations in the microgrid. The proposed control synthesis has considerable advantages over the trail-and-error-based tuning of a fixed structure controller presented in [15],

where the controller is limited to systems with one voltage regulator or multiple identical voltage regulators; on the other hand, the systematic control synthesis presented in this paper allows for one-step design of VFC for all (potentially heterogeneous) voltage regulators. In Section III, various structures of VFC are designed, including both SISO and MIMO controllers, and their closed-loop performance and robustness are compared via extensive simulations on a modified CIGRE test system to identify the most effective, practical, and computationally efficient control framework. Finally, Section IV highlights the main conclusions and contributions of the presented work.

II. Optimal VFC Design Problem

A. VFC Design

A balanced three-phase AC microgrid with synchronous machines [22], grid-following power converters [23], and exponential static load models [24] is considered here to represent a typical microgrid. The microgrid model receives the supplementary control signal $v_{\rm ref}$ and the load disturbance $S^{\rm ld}$; the model output is the machines angular frequency $\omega^{\rm sg}$. Thus, the overall open-loop linearized microgrid model can be described as follows:

$$\begin{aligned}\Delta\dot{x}^{\rm mg} &= A^{\rm mg}\Delta x^{\rm mg} + B_S^{\rm mg}\Delta S^{\rm ld} + B_v^{\rm mg}\Delta v_{\rm ref}\\ \Delta\omega^{\rm sg} &= C^{\rm mg}\Delta x^{\rm mg}\end{aligned} \tag{1}$$

where $x^{\rm mg}$ contains the machines, inverters, and network states, with the linear matrices $A^{\rm mg}$, $B_S^{\rm mg}$, $B_v^{\rm mg}$, and $C^{\rm mg}$ accordingly.

The guiding principle behind VFC is to measure the frequency deviations $\Delta\omega^{\rm sg}$ and change the set-points of voltage regulators in the system, to compensate for active power mismatches [15]. For example, in an event of under-frequency, the voltage regulator set-points are decreased, causing a decrease in the provided load voltage, and a subsequent decrease in load power consumption. For a typical load voltage sensitivity for islanded microgrids [15], [17], a 5% drop in the nominal operating voltage yields a 7.6% drop in the demand.

The design of VFC is formulated here as an optimal control problem for a so-called generalized plant $\mathcal{G}$, which is the model within the dashed box in Fig. 1. The generalized plant consists of the linearized microgrid model (3) augmented by the following additional equations:

(i) *Control signals*: $\Delta u = \Delta v_{\rm ref}$ generated by the VFC.

(ii) *Frequency measurement equations*: $\Delta y = \Delta\omega^{\rm sg} + W_n\Delta d_n$, where $\Delta d_n \in \mathbb{R}^{n_{\rm sg}}$ models measurement noise and $W_d = \mathrm{diag}(W_{d,1},\ldots,W_{d,n_{\rm sg}})$ is a diagonal matrix parameterizing the noise level.

(iii) *Load disturbance inputs*: parameterized as $\Delta S^{\rm ld} = W_S\Delta d_S$, where $d_S \in \mathbb{R}^{2n_{\rm ld}}$ models the load power disturbances and $W_S = \mathrm{diag}(W_{S,1},\ldots,W_{S,2n_{\rm ld}})$ parameterizes the disturbance strengths.

(iv) *System performance outputs*:

$$\begin{aligned}\Delta z = \mathrm{col}(\Delta z_1,\ldots,&\Delta z_{m+1}) =\\ &\mathrm{col}(W_\omega\Delta\omega^{\rm sg}, W_u\Delta u)\end{aligned} \tag{2}$$

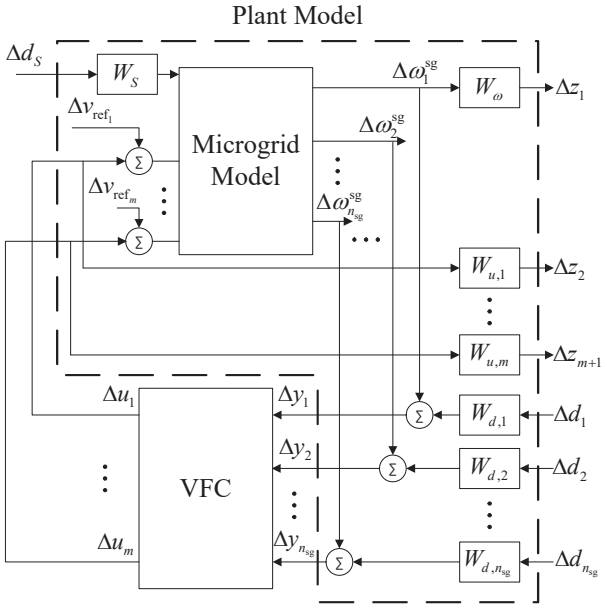

Fig. 1: Systematic VFC Control Synthesis Structure.

which contains the set of variables that one wishes the controller to "keep small" in the presence of disturbances, once again weighted using diagonal matrices W_ω and W_u of appropriate sizes. Note that the notation $\mathrm{col}(\Delta z_1,\ldots,\Delta z_{m+1})$ denotes the stacked column matrix of all entries[1].

In terms of these definitions and the microgrid model (3), the generalized plant $\mathcal{G}$ is given by:

$$\left[\begin{array}{c}\Delta\dot{x}^{\rm mg}\\ \hline \Delta z_1\\ \Delta z_2\\ \hline \Delta y\end{array}\right] = \left[\begin{array}{c|c|c|c} A^{\rm mg} & B_S^{\rm mg}W_S & \mathbb{0} & B_v^{\rm mg}\\ \hline W_\omega C^{\rm mg} & \mathbb{0} & \mathbb{0} & \mathbb{0}\\ \mathbb{0} & \mathbb{0} & \mathbb{0} & W_u\\ \hline C^{\rm mg} & \mathbb{0} & W_n & \mathbb{0}\end{array}\right]\left[\begin{array}{c}\Delta x^{\rm mg}\\ \hline \Delta d_S\\ \Delta d_n\\ \hline \Delta u\end{array}\right] \tag{3}$$

The problem of VFC design may then be posed as designing a linear time-invariant (LTI) feedback controller $\mathcal{K}$ with state $\xi(t)$:

$$\mathcal{K}: \quad \begin{aligned}\dot{\xi}(t) &= A_{\rm c}\xi(t) + B_{\rm c}\Delta y(t)\\ \Delta u(t) &= C_{\rm c}\xi(t) + D_{\rm c}\Delta y(t)\end{aligned} \tag{4}$$

processing noisy frequency measurements Δy and producing voltage regulator set points Δu, such that, when $\mathcal{K}$ is interconnected with the generalized plant $\mathcal{G}$, the influence of disturbances Δd on the performance variable Δz is minimized. The feedback interconnection is denoted by $\mathcal{F}(\mathcal{G},\mathcal{K})$, which is

[1]While it is intuitive that the VFC should keep the frequency deviations $\Delta\omega^{\rm sg}$ small, the control inputs Δu must also be included in the performance output to curb overly aggressive control actions, as in a classical LQR control problem. The weights W_ω and W_u weigh the relative sizes of these contributions to the overall size $\|\Delta z\|_2$ of the performance output.

again an LTI system with input Δd and output Δz, seeking to minimize the $\mathcal{H}_\infty$ norm of $\mathcal{F}(\mathcal{G},\mathcal{K})$, which is defined as the maximum energy amplification from Δd to Δz as follows:

$$\|\mathcal{F}(\mathcal{G},\mathcal{K})\|_{\mathcal{H}_\infty} := \sup_{\Delta d\in\mathscr{L}_2,\Delta d\neq 0} \frac{\|\Delta z\|_{\mathscr{L}_2}}{\|\Delta d\|_{\mathscr{L}_2}} \tag{5}$$

where $\|\Delta\eta\|_{\mathscr{L}_2} := \left(\int_0^\infty \|\Delta\eta(t)\|_2^2\,\mathrm{d}t\right)^{1/2}$ denotes the $\mathscr{L}_2$-norm of the signal $\Delta\eta(t)$ [25]. The (sub)-optimal $\mathcal{H}_\infty$ control problem is then formulated as:

$$\underset{\mathcal{K}}{\text{minimize}} \quad \gamma \qquad \text{subject to} \quad \|\mathcal{F}(\mathcal{G},\mathcal{K})\|_{\mathcal{H}_\infty} < \gamma\,. \tag{6}$$

Under standard technical assumptions [25], this minimization problem is well-posed and efficiently solvable via convex optimization.

B. Model Simplification

The optimal control synthesis discussed in Section II yields a VFC with the same number of states as the generalized plant [25]. This can be computationally expensive, and implementing a high-order VFC is difficult in practice, thus it is desirable to reduce the dimensionality of the plant when possible [26]. Luckily, the physical properties typical of most microgrids allow for a natural hierarchical or reduced-order models that approximate well the original model for the purposes of VFC design.

It has been posed that the network in microgrids may not play a significant role in the performance of control and optimization techniques [19], in particular because feeders are short and their capacity is much greater than the maximum system demand [20], [21]. Furthermore, the design of an effective VFC is largely informed by load voltage sensitivity and voltage and frequency control (such as exciter and governor) parameters, and not by network dynamics, topology, or impedance. Hence, it is argued next that the static network model may be removed, effectively reducing the microgrid to a single bus.

1) Elimination of Feeders: If the feeders are short and have low impedance, all points in the network are very close electrically. Practice shows that the voltage drop along a microgrid feeder rarely exceeds 0.02 pu in isolated/islanded microgrids [19]–[21]. Therefore, as the principle of VFC is to adjust voltage levels at loads by modifying the voltage at the point of regulation, the feeders will have negligible impact on VFC performance.

To validate this idea dynamically, a modified version of the CIGRE benchmark for medium voltage distribution network in [27] shown in Fig. 3 is used as the test system, with the original feeder and load parameters. The system has three diesel synchronous machine S1, S2, and S3, with a rating of 1.42, 0.86, and 0.57 MVA, respectively. The diesel-based synchronous machines and governors are tuned and validated according the actual measurements from commercial grade synchronous machines in [28]; the governors are modeled using the model depicted in in Fig. **??**, and the voltage regulators and exciters are represented using the simplified transfer function $1/(K_E + T_E s)$ to reduce complexity. The

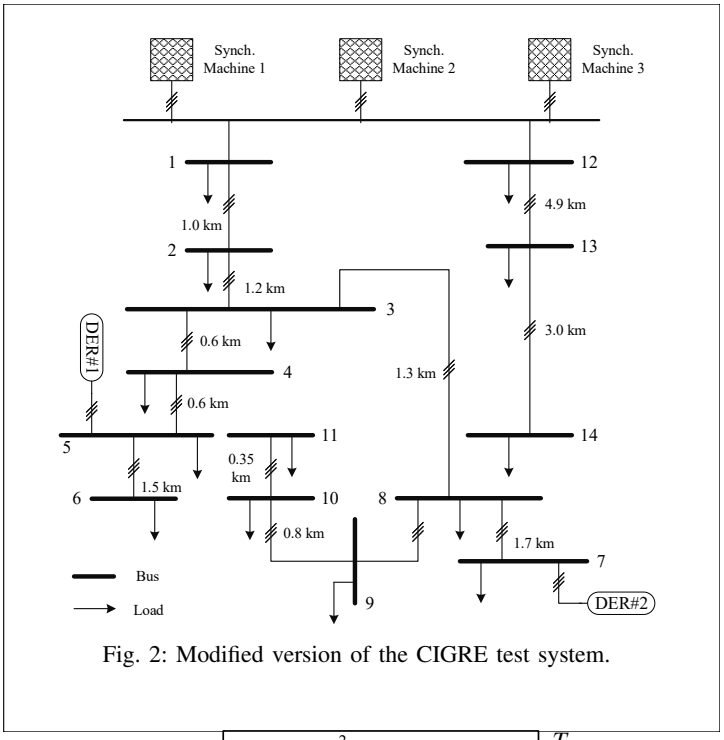

Fig. 2: Modified version of the CIGRE test system.

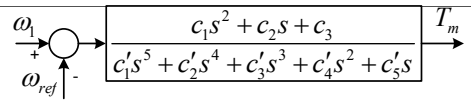

Fig. 3: Diesel generator model [29].

machine and associated controls parameters are presented in Table **??**. In addition, the system has two 1 MW inverters, whose parameters are provided in Table **??**, operating in grid-feeding mode. Loads are modeled using a voltage-sensitive exponential model with a 1.5 exponent, which is a reasonable value for typical isolated microgrids [17].

Based on the microgrid model (3) and computing the Fourier-domain response of the machine frequencies to the voltage regulator setpoints, one has:

$$\begin{aligned}\Delta\omega^{\mathrm{sg}}(\mathbf{j}\omega) &= \left[C^{\mathrm{mg}}(\mathbf{j}\omega I - A^{\mathrm{mg}})^{-1}B_v^{\mathrm{mg}}\right]\Delta v_{\mathrm{ref}}(\mathbf{j}\omega)\\ &= T_\epsilon(\mathbf{j}\omega)\Delta v_{\mathrm{ref}}(\mathbf{j}\omega)\,.\end{aligned} \tag{7}$$

Introducing a parameter $\epsilon \in [0,1]$ that multiplies the feeder impedances; thus, if $\epsilon = 0$, the feeders are removed, while $\epsilon = 1$ yields the original model. The frequency response of the system with feeders ($\epsilon = 1$) and without feeders ($\epsilon = 0$) is illustrated in Fig. 4, for the parameters of the CIGRE benchmark system [27], which exhibits relatively long feeders (close to 12 km from the PCC to the furthest load). Observe that the response of the system with and without the inclusion of feeders is nearly identical in a frequency range considerably larger than the VFC intended bandwidth. For this figure, the test system has three inputs, which are deviations to the synchronous machines voltage exciter set-points, and one output, which is the system global frequency.

2) Balanced Model Truncation: After eliminating the feeders, the standard model reduction technique of balanced trun-

TABLE I: Diesel generator parameters.

Param.	Value		
	S.M. 1	S. M. 2	S.M. 3
S_b kVA	1,420	860	570
R_s pu	0.0052	0.0052	0.0052
X_l pu	0.063	0.023	0.021
X_d pu	1.91	1.75	1.7479
X'_d pu	0.1318	0.0755	0.082
X''_d pu	0.092	0.0521	0.0706
X_q pu	0.96	1.2569	1.1516
X'_q pu	0.628	0.898	0.828
X''_q pu	0.122	0.1483	0.1307
T'_d s	3.03	2.115	2.115
T''_d s	0.054	0.054	0.054
T'_q s	0.85	0.85	0.85
T''_q s	0.05	0.05	0.05
H s	0.5134	0.5134	0.5134
K_E	0.0133	0.02	0.0286
T_E	0.00016	0.00031	0.00057
c_1	36944	36944	36944
c_2	202777	202777	202777
c_3	277777	277777	277777
c'_1	3e-5	3e-5	3e-5
c'_2	0.047	0.047	0.047
c'_3	19.66	19.66	19.66
c'_4	1944	1944	1944
c'_5	55555	55555	55555

TABLE II: DER inverter parameters.

L_f	R_f	C_f	R_d	$V_{rateddc}$
0.166 mH	4.2 mΩ	626.8 μF	84.7 mΩ	750 v
C_{dclink}	R_B	L_{chopf}	f_s	V_{RMSL-L}
20 mF	0.2 Ω	3.3 mH	3 kHz	460 v

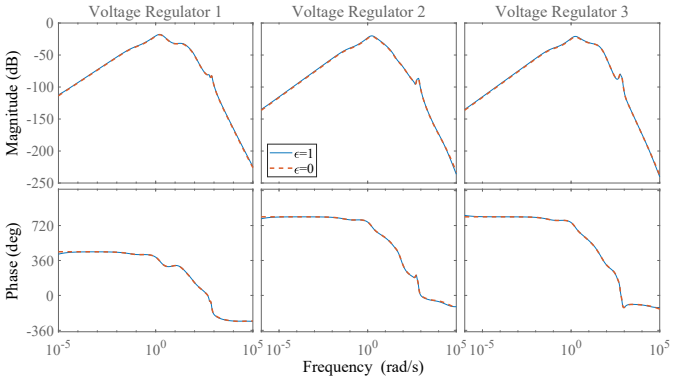

Fig. 4: Frequency response $T_\epsilon(\mathbf{j}\omega)$ for the CIGRE test system with $\epsilon \in \{0, 1\}$.

cation is applied to obtain a reduced-order LTI model which describes the input-output dynamics of the microgrid. The order of the reduced model is chosen to obtain a good match between the frequency responses of the reduced and full-order models based on [25].

For the test system presented in this paper, the full model order is 117 and is reduced to 10 for controller synthesis. This is chosen based on the desired bandwidth of the closed loop plant with the VFC control, and the frequency response of the reduced-order model, as shown in Fig. 5. Given that the VFC is primarily intended to compensate for power mismatches rather

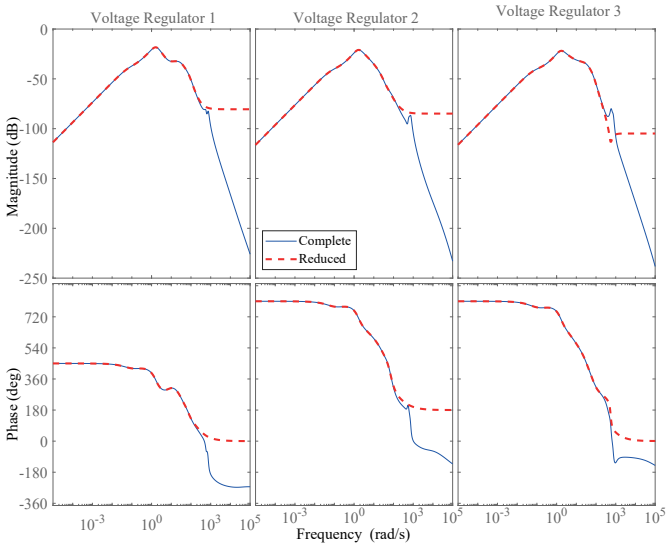

Fig. 5: Frequency response $T_\epsilon(\mathbf{j}\omega)$ for the CIGRE test system with no feeders and the reduced-order version of it.

than damping fast oscillations, the frequency range of interest is well below 1000 rad/s, within which the frequency response of the reduced-order plant is nearly identical.

III. Simulation Results

This section illustrates the VFC control performance, and evaluates the impact of system simplifications during the design process. The test system shown in Fig. 3 is also used in this Section. To illustrate the flexibility of the VFC control architecture, two VFC designs are considered here. The first design is a standard centralized controller, which processes the frequency measurements from all three synchronous machines, and produces voltage reference changes for the three corresponding exciter systems (a 3×3 controller). The second design also produces three exciter set-points, but only processes the frequency deviation from synchronous machine 1 (a 3×1 controller). For implementation, if the empirical fact that frequency is a global variable in isolated microgrids is exploited (negligible differences throughout the system), one may decentralize this design by letting each unit compute the corresponding regulator setpoint using its own frequency deviation instead of that from unit S1:

$$\begin{bmatrix} \mathcal{K}_{11} \\ \mathcal{K}_{21} \\ \mathcal{K}_{31} \end{bmatrix} \approx \begin{bmatrix} \mathcal{K}_{11} & 0 & 0 \\ 0 & \mathcal{K}_{21} & 0 \\ 0 & 0 & \mathcal{K}_{31} \end{bmatrix}$$

This design is referred to as the decentralized VFC design.

The model simplifications explained in Section II-B are applied to the system, thus reducing the overall system states from 117 to 10. The control synthesis is performed using MATLAB built-in H infinity synthesis function [30], resulting in a controller with 10 states. Finally, for the sake of comparison, the performance of a single-input-single-output PI-based VFC design, as shown in Fig. 6, is also included in the result. The feedback loop in Fig. 6 mitigates possible oscillations caused

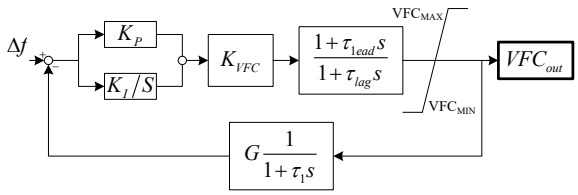

Fig. 6: PI-based VFC based on [15].

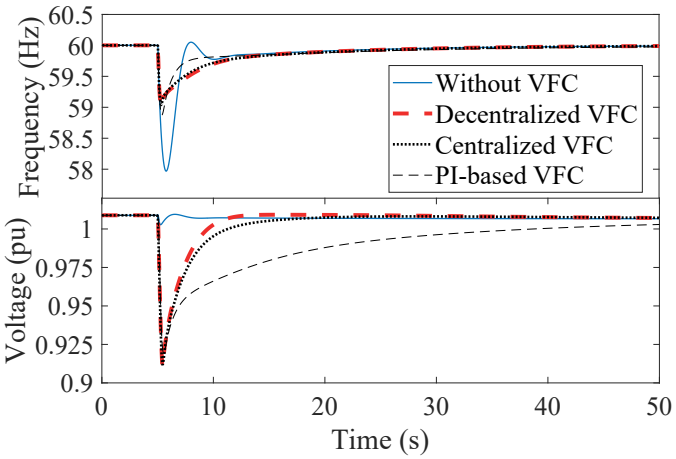

Fig. 7: Frequency and voltage response of the system with and without the VFC.

by interaction of the VFC and governors integrators. This PI-based VFC receives the frequency deviation from S1 and sends the same output signal to all the three exciters, and is tuned by a combination of Ziegler-Nichols and grid-search techniques.

To investigate the impact of VFC, the system loading is suddenly and uniformly increased by 650 kW, and the system performance with and without VFC is shown in Fig. 7. Prior to the disturbance, the system nominal loading is 2.5 MW of active power and 1 MVar of reactive power. The inverters are injecting a total of 1 MW of active power and 600 kVar of reactive power. S1 is operating in isochronous mode, injecting 625 kW and 480 kVar, while S2 and S3 are operating in constant active power mode, injecting of 548 kW and 440 kW active power correspondingly.

As seen in Fig. 7, the system frequency response is considerably improved, with over 50% decrease in the peak-to-peak value. Moreover, the system damping is also enhanced, as the system with VFC exhibits a critically damped performance. In addition, the steady-state deviation for both voltage and frequency is zero. Although the frequency response with the PI-based VFC has a slightly shorter recovery time, the voltage recovery is considerably slower, demonstrating the major advantage of the design proposed here as compared to a conventional PI-based VFC. Note that the difference between the performance of the two proposed VFC designs is not significant, verifying the adequacy of the decentralized design and perhaps its superiority as there is no need of communication among the machines. The results presented here demonstrate the considerable benefit of a well-tuned VFC,

TABLE III: Eigenvalues and damping ratios of the system with and without VFC.

Without	Centralized	Decentralized	PI-based
-0.0709	-0.0829	-0.0767	-0.0548
-0.1951	-0.0999	-0.1232	-0.1945
-0.8828±1.4117i	-0.1932	-0.1936	-0.2055±0.134i
0.531			0.838
-1.1465	-0.661±0.152i	-0.508±0.295i	-1.144
	0.975	0.865	
-1.1706	-1.1466	-1.1424	-1.1689

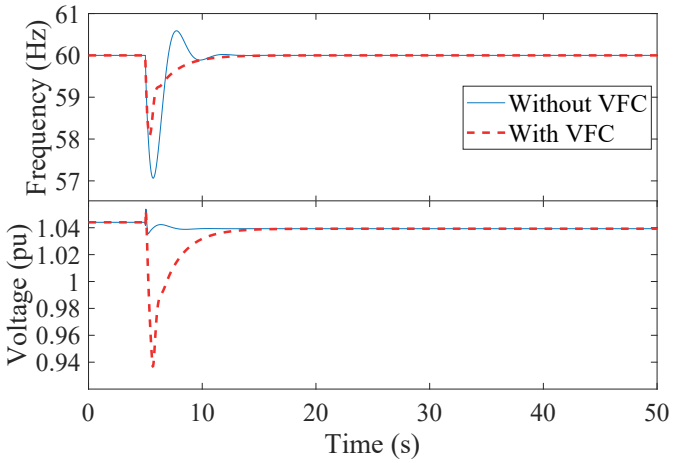

Fig. 8: Frequency and voltage response of the system with and without the VFC with grid supporting converter.

acting as a virtual flywheel in the system to compensate for transient active power mismatches in the system.

The impact of the controller on the system eigenvalues is reported in Table III, which includes the first 5 eigenvalues closest to the imaginary axis. Observe for the centralized and decentralized VFCs that the system critical eigenvalues are slightly more negative and the damping ratios are larger, indicating improved system stability.

To further verify the controller synthesis procedure, S2 and S3 are both replaced by a 1 MW grid-supporting inverter. The inverter is set to inject the same active power as S1 and 100 KVar at nominal steady-state terminal voltage. The inverter reactive power injection is sensitive to a terminal voltage set-point through a 1.42 MVar/pu linear droop mechanism. The rest of the system, including the loading and the disturbance is the same as before. Thus, the VFC in this case has one input, S1 frequency, and two outputs that integrate with S1 exciter set-point and the grid-supporting inverter voltage-set point. The system performance is shown in Fig. 8, demonstrating a considerable improvement in the system frequency response. This is also observed in the system three eigenvalues with the largest real-part shown in Table IV.

IV. Conclusions

A balanced three-phase AC microgrid model was used to demonstrate the insignificant impact of microgrid feeders on

TABLE IV: Eigenvalues and damping ratios of the system with grid-supporting converter with and without VFC.

Without VFC	with VFC
-0.8791±1.4824i	-0.6184
0.511	
-1.2003	-1.2026
-16.0883±13.3779i	-4.5233±4.834i
0.769	0.683

voltage-frequency coupling through mathematical analysis and simulations; the outcome of this analysis laid the foundation for considerable model simplification. An optimal $\mathcal{H}_\infty$ control synthesis framework for VFC was established on the simplified model and tested on the actual model, showing that the synthesis process is robust to model simplifications, and that a well-tuned VFC controller enhances the system damping, as well as its frequency response. Thus, the VFC plays the role of a virtual flywheel with a considerably capacity compared to the system nominal rating. The presented results here illustrate the small role of microgrid feeder on its static and dynamic performance, as well as voltage-frequency coupling. Furthermore, the presented study lays the foundation on an even more robust VFC designs, considering uncertainty in load and DERs parameters.

REFERENCES

[1] B. Lasseter, "Microgrids [distributed power generation]," in *Proc. of IEEE Power Eng. Soc. Winter Meet.*, Jan. 2001, pp. 146–149.

[2] R. H. Lasseter, J. H. Eto, B. Schenkman, J. Stevens, H. Vollkommer, D. Klapp, E. Linton, H. Hurtado, and J. Roy, "CERTS microgrid laboratory test bed," *IEEE Trans. Power Del.*, vol. 26, pp. 325–332, Jan. 2011.

[3] F. Katiraei, M. Iravani, and P. W. Lehn, "Micro-grid autonomous operation during and subsequent to islanding process," *IEEE Trans. Power Del.*, vol. 20, no. 1, pp. 248–257, Jan. 2005.

[4] D. E. Olivares, A. Mehrizi-Sani, A. H. Etemadi, C. A. Cañizares, R. Iravani, M. Kazerani, A. H. Hajimiragha, O. Gomis-Bellmunt, M. Saeedifard, R. Palma-Behnke, G. A. Jimenez-Estevez, and N. D. Hatziargyriou, "Trends in microgrid control," *IEEE Trans. Smart Grid*, vol. 5, no. 4, pp. 1905–1919, July 2014.

[5] M. Farrokhabadi, C. A. Cañizares, J. W. Simpson-Porco, E. Nasr, L. Fan, P. A. Mendoza Araya, R. Tonkoski, U. Tamrakar, N. Hatziargyriou, D. Lagos, R. W. Wies, M. Paolone, M. Liserre, L. Meegahapola, M. Kabalan, A. H. Hajimiragha, D. Peralta, M. Elizondo, K. P. Schneider, F. Tuffner, J. Reilly, and R. Palma Behnke, "Microgrid stability, definitions, analysis, and modeling," IEEE Power and Energy Society, Tech. Rep., Apr. 2018.

[6] G. Dellile, B. Francois, and G. Malarange, "Dynamic frequency control support by energy storage to reduce the impact of wind and solar generation on isolated power system's inertia," *IEEE Trans. Sustain. Energy*, vol. 3, no. 4, pp. 931–939, Oct. 2012.

[7] A. H. Hajimiragha, M. R. Dadash Zadeh, and S. Moazeni, "Microgrids frequency control considerations within the framework of the optimal generation scheduling problem," *IEEE Trans. Smart Grid*, vol. 6, no. 2, pp. 534–547, Mar. 2015.

[8] J. M. Guerrero, M. Chandorka, T. Lee, and P. C. Loh, "Advanced control architectures for intelligent microgrids–part I: Decentralized and hierarchical control," *IEEE Trans. Ind. Electron.*, vol. 60, no. 4, pp. 1254–1262, April 2012.

[9] J. M. Guerrero, P. C. Loh, T. Lee, and M. Chandorkar, "Advanced control architectures for intelligent microgrids–part II: Power quality, energy storage, and AC/DC microgrids," *IEEE Trans. Ind. Electron.*, vol. 60, no. 4, pp. 1263–1270, April 2012.

[10] R. Majumder, G. Ledwich, A. Ghosh, S. Chakrabarti, and F. Zare, "Droop control of converter-interfaced microsources in rural distributed generation," *IEEE Trans. Power Del.*, vol. 25, no. 4, pp. 2768–2778, March 2010.

[11] Y. A.-R. I. Mohamed and E. F. El-Saadany, "Adaptive decentralized droop controller to preserve power sharing stability of paralleled inverters in distributed generation microgrids," *IEEE Trans. Power Electron.*, vol. 23, no. 6, pp. 2806–2816, Nov. 2008.

[12] Y. Xu, W. Zhang, G. Hug, S. Kar, and Z. Li, "Cooperative control of distributed energy storage systems in a microgrid," *IEEE Trans. Smart Grid*, vol. 6, no. 1, pp. 238–248, Jan. 2015.

[13] A. H. Etemadi, E. J. Davison, and R. Iravani, "A decentralized robust control strategy for multi-der microgrids—part I: Fundamental concepts," *IEEE Trans. Power Del.*, vol. 27, no. 4, pp. 1843–1853, Oct. 2012.

[14] Q. Lv, G. Yang, H. Geng, and X. Zhang, "Hybrid cooperative control method for microgrid with large generation or load fluctuations," *The Journal of Engineering*, vol. 2017, no. 13, pp. 1896–1900, Oct. 2017.

[15] M. Farrokhabadi, C. A. Cañizares, and K. Bhattacharya, "Frequency control in isolated/islanded microgrids through voltage regulation," *IEEE Trans. Smart Grid*, vol. 8, no. 3, pp. 1185–1194, Oct. 2015.

[16] M. Farrokhabadi, C. A. Cañizares, and K. Bhattacharya, "A voltage-based frequency controller for inverter-based systems in microgrids," in *Proc. IEEE Power Eng. Soc. Gen. Meeting*, Boston, MA, July 2016, pp. 1–5.

[17] G. Delille, L. Capely, D. Souque, and C. Ferrouillat, "Experimental validation of a novel approach to stabilize power system frequency by taking advantage of load voltage sensitivity," in *Proc. of IEEE PowerTech.*, Eindhoven, Netherlands, June 2015.

[18] M. Diaz-Aguilo, J. Sandraz, R. Macwan, F. de Leon, D. Czarkowski, C. Comack, and D. Wang, "Field-validated load model for the analysis of CVR in distribution secondary networks: Energy conservation," *IEEE Trans. Power Del.*, vol. 28, no. 4, pp. 2428 – 2436, Oct. 2013.

[19] B. V. Solanki, C. A. Canizares, and K. Bhattacharya, "Practical energy management systems for isolated microgrids," *IEEE Trans. Smart Grid*, vol. 10, no. 5, pp. 4762–4775', Sept. 2019.

[20] R. Palma-Behnke, C. Benavides, F. Lanas, B. Severino, L. Reyes, J. Llanos, and D. Saez, "A microgrid energy management system based on the rolling horizon strategy," *IEEE Trans. Smart Grid*, vol. 4, no. 2, pp. 996–1006, June 2013.

[21] A. H. Hajimiragha and M. R. D. Zadeh, "Research and development of a microgrid control and monitoring system for the remote community of Bella Coola: Challenges, solutions, achievements and lessons learned," in *Proc. IEEE Int. Conf. on Smart Energy Grid Eng. (SEGE)*, Oshawa, Canada, Aug. 2001.

[22] P. C. Krause, O. Wasynczuk, and S. D. Sudhoff, *Analysis of Electric Machinery and Drive Systems*. Piscatawar, NJ: IEEE Press, 2002.

[23] M. Farrokhabadi, S. König, C. A. Cañizares, K. Bhattacharya, and T. Leibfired, "Battery energy storage system models for microgrid stability analysis and dynamic simulation," *IEEE Trans. Power Syst.*, vol. 33, no. 2, pp. 2301–2312, Mar. 2018.

[24] F. Katiraei, M. Iravani, and P. Lehn, "Small-signal dynamic model of a micro-grid including conventional and electronically interfaced distributed resources," *IET Gen. Trans. Dist.*, vol. 1, no. 3, pp. 369 – 378, May 2017.

[25] G. E. Dullerud and F. Paganini, *A Course in Robust Control Theory*, ser. Texts in Applied Mathematics. Springer-Verlag, 2000, no. 36.

[26] D. Henrion, "H-infinity controller design on the compleib problems with the robust control toolbox for matlab," LAAS-CNRS Research Report, Tech. Rep., Oct. 2005.

[27] K. Strunz, E. Abbasi, C. Abbey, C. Andrieu, U. Annakkage, S. Barsali, R. C. Campbell, R. Fletcher, F. Gao, T. Gaunt, A. Gole, N. Hatziargyriou, R. Iravani, G. Joos, H. Konishi, M. Kuschke, E. Lakervi, C. Liu, J. Mahseredjian, F. Mosallat, D. Muthumuni, A. Orths, S. Papathanassiou, K. Rudion, Z. Styczynski, and S. C. Verma, "Benchmark systems for network integration of renewable and distributed energy resources," Cigre Task Force C6.04.02, Tech. Rep., May 2013.

[28] M. Arriaga and C. A. Cañizares, "Overview and analysis of data for microgrid at kasabonika lake first nation (KLFN)," Hatch Project Confidential Report, University of Waterloo, Tech. Rep., Sep. 2015.

[29] NEPLAN, "Turbine-governor models," Sept. 2015. [Online]. Available: https://www.neplan.ch/wp-content/uploads/2015/08/Nep_TURBINES_GOV.pdf

[30] "h2hinfsyn." [Online]. Available: https://www.mathworks.com/help/robust/ref/h2hinfsyn.html